

Synthesis, Structure, and Redox Chemistry of Heteropolymetallic Carbon Complexes with MC_2M' , MC_4M' , and $MC_4M'C_4M$ Linkages. Transmetalations of Lithiocarbon Complexes ($\eta^5\text{-C}_5\text{Me}_5\text{Re}(\text{NO})(\text{PPh}_3)(\text{C}\equiv\text{CLi})$ and ($\eta^5\text{-C}_5\text{Me}_5\text{Re}(\text{NO})(\text{PPh}_3)(\text{C}\equiv\text{CC}\equiv\text{CLi})$)

Weiqing Weng, Tamás Bartik, Monika Brady, Berit Bartik, James A. Ramsden, Atta M. Arif, and J. A. Gladysz*

Contribution from the Department of Chemistry, University of Utah, Salt Lake City, Utah 84112

Received July 31, 1995[®]

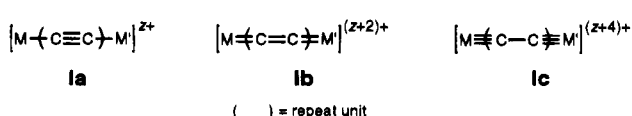
Abstract: Reactions of $(\eta^5\text{-C}_5\text{Me}_5)\text{Re}(\text{NO})(\text{PPh}_3)(\text{C}\equiv\text{CLi})$ and *trans*-Pd(PEt₃)₂(Cl)₂ or *trans*-Rh(PPh₃)₂(CO)(Cl) give heterobimetallic C₂ complexes *trans*- $(\eta^5\text{-C}_5\text{Me}_5)\text{Re}(\text{NO})(\text{PPh}_3)(\text{C}\equiv\text{C})\text{Pd}(\text{PEt}_3)_2(\text{Cl})$ (**3**, 66%) or *trans*- $(\eta^5\text{-C}_5\text{Me}_5)\text{Re}(\text{NO})(\text{PPh}_3)(\text{C}\equiv\text{C})\text{Rh}(\text{PPh}_3)_2(\text{CO})$ (**4**, 72%). Reaction of $[(\eta^5\text{-C}_5\text{Me}_5)\text{Re}(\text{NO})(\text{PPh}_3)(\text{ClC}_6\text{H}_5)]^+$ BF₄⁻ and HC≡CC≡CSiMe₃ gives $[(\eta^5\text{-C}_5\text{Me}_5)\text{Re}(\text{NO})(\text{PPh}_3)(\text{HC}\equiv\text{CC}\equiv\text{CSiMe}_3)]^+$ BF₄⁻ (93%; HC≡C ligated), which with *t*-BuOK and K₂CO₃/MeOH yields $(\eta^5\text{-C}_5\text{Me}_5)\text{Re}(\text{NO})(\text{PPh}_3)(\text{C}\equiv\text{CC}\equiv\text{CH})$ (**9**, 84%). Reaction of **9** and *n*-BuLi gives $(\eta^5\text{-C}_5\text{Me}_5)\text{Re}(\text{NO})(\text{PPh}_3)(\text{C}\equiv\text{CC}\equiv\text{CLi})$ (**10**), which is trapped by MeI as $(\eta^5\text{-C}_5\text{Me}_5)\text{Re}(\text{NO})(\text{PPh}_3)(\text{C}\equiv\text{CC}\equiv\text{CMe})$ (85%). Reaction of **10** and *trans*-Pd(PEt₃)₂(Cl)₂ (2:1) gives *trans*- $(\eta^5\text{-C}_5\text{Me}_5)\text{Re}(\text{NO})(\text{PPh}_3)(\text{C}\equiv\text{CC}\equiv\text{C})\text{Pd}(\text{PEt}_3)_2(\text{C}\equiv\text{CC}\equiv\text{C})(\text{Ph}_3\text{P})(\text{ON})\text{Re}(\eta^5\text{-C}_5\text{Me}_5)$ (**12**, 73%). At a 1:1 stoichiometry, *trans*- $(\eta^5\text{-C}_5\text{Me}_5)\text{Re}(\text{NO})(\text{PPh}_3)(\text{C}\equiv\text{CC}\equiv\text{C})\text{Pd}(\text{PEt}_3)_2(\text{Cl})$ (**13**) is the major product. Cyclic voltammograms of **3**, **12**, and **13** show reversible one-electron oxidations. Reactions of **3** and **12** with $(\eta^5\text{-C}_5\text{H}_5)_2\text{Fe}^{\bullet+}\text{PF}_6^-$ give the radical cations **3**⁺ PF₆⁻ and **12**⁺ PF₆⁻. These are unstable at room temperature, but ESR data show the odd electrons to be localized on (one) rhenium. Complexes **3** and **4** (but not **12** and **13**) exhibit restricted rotation about the Re_xM moiety, as evidenced by two R₃PMR₃³¹P NMR signals at low temperature ($\Delta G^\ddagger(T_c) = 11.7\text{--}10.9$ kcal/mol). The crystal structure of **3** shows eclipsed PEt₃ ligands.

Transition metals provide a unique means of stabilizing reactive elemental carbon fragments or allotropes.¹⁻³ Such complexes have recently attracted considerable attention from both fundamental and applied viewpoints. Some exhibit potentially useful materials properties.^{1a} Others provide models for carbide species that are generated on heterogeneous catalysts used in processing basic chemical feedstocks.^{2b,4} Many also have a purely aesthetic appeal.

One major objective has been the preparation of compounds in which sp carbon chains span two metals, $L_nM(C)_xM'L'_n$ (I).¹ There are now many examples of such C_2 complexes.⁵ However, higher homologs remain much less well explored.^{6,7}

Importantly, the structures of both diamond and graphite must terminate with non-carbon substituents. Thus, at very high values of x , I can similarly be viewed as a carbon allotrope.⁸

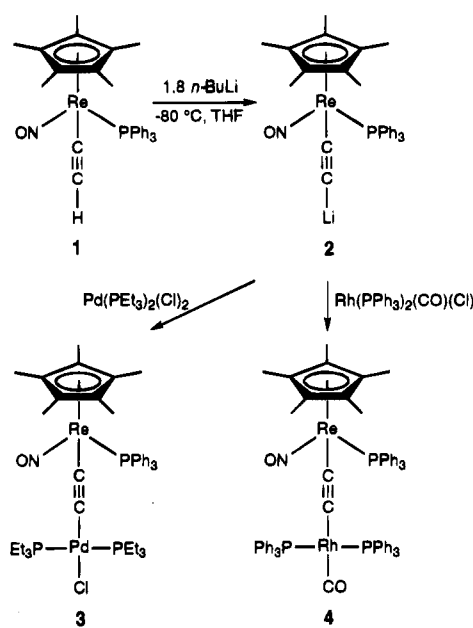
We have been particularly attracted by the potential for charge transfer phenomena involving the metal termini in **I**. These would include optical transitions and nonlinearities and electron delocalization in radical ions. Such properties reflect the abilities of these unsaturated, wire-like assemblies to serve as "conductors", and could be investigated as a function of carbon chain length. Note that with even-numbered carbon chains, valence types **Ia**, **Ib**, or **Ic** are possible. These are formally related by two-electron oxidations or reductions. Alternatively, the electron-paired formulae depicted may be excited states as opposed to ground states. Surprisingly, only a few complexes have been characterized in more than one redox state ^{6,1}



Several strategies have been utilized to prepare complexes of the type **I**. However, we felt that the deprotonation of ethynyl complexes $L_nMC\equiv CH$, or higher homologs, should afford nucleophilic conjugate bases that would allow syntheses of previously inaccessible classes of adducts. Thus, reactions of chiral rhodium ethynyl complexes of the formula $(n^5-C_5R_5)Re$

(7) Partially characterized C₆ and C₈ complexes: Kim, P. J.; Masai, H.; Sonogahira, K.; Hagihara, N. *Inorg. Nucl. Chem. Lett.* **1970**, 181.

(8) Lagow, R. J.; Kampa, J. J.; Wei, H.-C.; Battle, S. L.; Genge, J. W.; Laude, D. A.; Harper, C. J.; Bau, R.; Stevens, R. C.; Haw, J. F.; Munson, E. *Science* **1995**, 267, 362.

Scheme 1. Syntheses of ReC_2M Complexes

(NO)(PPh₃)(C≡CH) (R = H, Me) and *n*-BuLi were examined. In a previous full paper,⁹ we detailed the generation of the corresponding $\text{ReC}\equiv\text{CLi}$ species, and reactions with carbon, silicon, and tin electrophiles.

As described in earlier communications,¹⁰ such species have allowed access to a variety of complexes of the type I.¹¹ Indeed, there appears to be no upper limit on chain length for valence type Ia.¹² Thus, we report in this full paper, which represents the first in a series, the application of our methodology to ReC_2M , ReC_4M , and $\text{ReC}_4\text{MC}_4\text{Re}$ complexes, including radical cations generated in subsequent oxidations. Extensions to ReC_3M and ReC_5M complexes are detailed in a companion manuscript.¹³ Prior efforts by Wong involving $\text{FeC}\equiv\text{CC}\equiv\text{CLi}$ species,^{6b} and Hagiwara involving $\text{PdC}_4\text{MC}_4\text{Pd}$ complexes,^{6a} also deserve emphasis, and are described in the Discussion Section.

Results

1. Syntheses of ReC_2M Complexes. As shown in Scheme 1, the pentamethylcyclopentadienyl ethynyl complex ($\eta^5\text{-C}_5\text{Me}_5$) $\text{Re}(\text{NO})(\text{PPh}_3)(\text{C}\equiv\text{CH})$ (**1**) was treated with *n*-BuLi (1.8 equiv) in THF at -80°C . This generated the $\text{ReC}\equiv\text{CLi}$ species ($\eta^5\text{-C}_5\text{Me}_5$) $\text{Re}(\text{NO})(\text{PPh}_3)(\text{C}\equiv\text{CLi})$ (**2**) as previously described.⁹ In separate experiments, the palladium¹⁴ and rhodium¹⁵ chloride complexes *trans*- $\text{Pd}(\text{PEt}_3)_2(\text{Cl})_2$ and *trans*- $\text{Rh}(\text{PPh}_3)_2(\text{CO})(\text{Cl})$ were added (1.1–1.2 equiv). Workups gave the red heterobimetallic ReC_2M complexes *trans*-($\eta^5\text{-C}_5\text{Me}_5$) $\text{Re}(\text{NO})(\text{PPh}_3)$

(9) Ramsden, J. A.; Weng, W.; Gladysz, J. A. *Organometallics* 1992, 11, 3635.

(10) (a) Ramsden, J. A.; Weng, W.; Arif, A. M.; Gladysz, J. A. *J. Am. Chem. Soc.* 1992, 114, 5890. (b) Weng, W.; Ramsden, J. A.; Arif, A. M.; Gladysz, J. A. *J. Am. Chem. Soc.* 1993, 115, 3824. (c) Weng, W.; Arif, A. M.; Gladysz, J. A. *Angew. Chem., Int. Ed. Engl.* 1993, 32, 891. (d) Weng, W.; Bartik, T.; Gladysz, J. A. *Angew. Chem., Int. Ed. Engl.* 1994, 33, 2199.

(11) Related syntheses involving direct oxidative couplings of ($\eta^5\text{-C}_5\text{Me}_5$) $\text{Re}(\text{NO})(\text{PPh}_3)(\text{C}\equiv\text{C})_n\text{H}$ species: (a) Zhou, Y.; Seyler, J. W.; Weng, W.; Arif, A. M.; Gladysz, J. A. *J. Am. Chem. Soc.* 1993, 115, 8509. (b) Seyler, J. W.; Weng, W.; Zhou, Y.; Arif, A. M.; Gladysz, J. A. *Organometallics* 1993, 12, 3802. (c) Brady, M.; Weng, W.; Gladysz, J. A. *J. Am. Chem. Soc., Chem. Commun.* 1994, 2655.

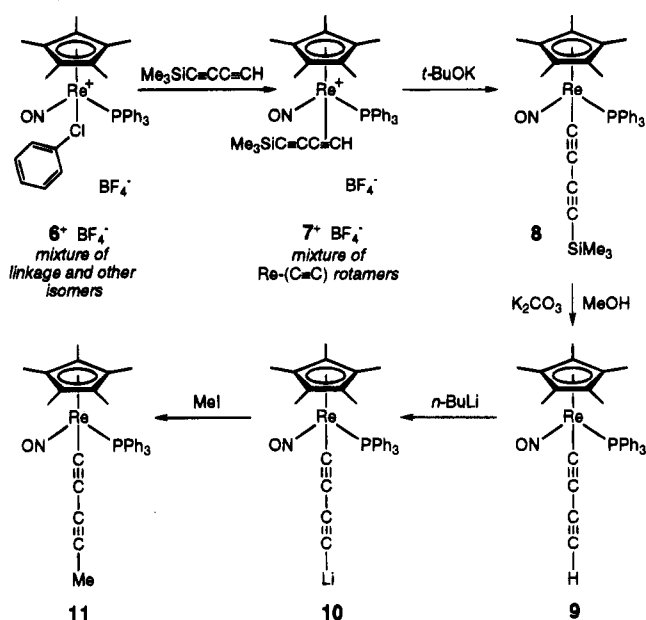
(12) Bartik, T.; Bartik, B.; Brady, M.; Dembinski, R.; Gladysz, J. A. Submitted for publication.

(13) Bartik, T.; Weng, W.; Ramsden, J. A.; Arif, A. M.; Gladysz, J. A. Full paper in preparation.

(14) Mann, F. G. *J. Chem. Soc.* 1935, 1549.

(15) Wilkinson, G. *Inorg. Synth.* 1968, 11, 99.

Scheme 2. Syntheses of 1,3-Butadiynyl and Related Complexes



(C≡C)Pd(PEt₃)₂(Cl) (**3**) and *trans*-($\eta^5\text{-C}_5\text{Me}_5$) $\text{Re}(\text{NO})(\text{PPh}_3)$ -(C≡C)Rh(PPh₃)₂(CO) (**4**) in 66–72% yields (Scheme 1). Hence, **2** can be derivatized with transition metal electrophiles.

Complexes **3** and **4** were stable as solids in air for months. However, **4** was somewhat labile in solution. A similar reaction of **2** and the rhenium bromide (CO)₅ReBr gave an unstable product that could not be unambiguously identified. In some cases, carbon nucleophiles preferentially attack the carbon monoxide ligands of this electrophile.¹⁶

Both **3** and **4**, and other new compounds isolated below, were characterized by microanalysis and IR, NMR (¹H, ¹³C, ³¹P), and mass spectroscopy. Data are summarized in the Experimental Section. The structural assignments were supported by numerous features. For example, mass spectra exhibited strong molecular ions, and ¹³C NMR spectra showed C≡C signals in typical chemical shift ranges (C₆D₆, ppm, ReC≡CM: **3**, 111.7/116.2; **4**, 134.6/153.4).⁹ Each C≡C signal of **3** was a doublet of triplets (*J* = 15.1/4.3 and 1.5/17.5 Hz), consistent with a PPh₃ ligand on rhenium and two *trans* PEt₃ ligands on palladium. IR spectra showed weak ν_{C≡C} bands (3/4 1989/2023 cm⁻¹), and a Raman spectrum of **3** gave a slightly shifted absorption (1971 cm⁻¹).

2. Synthesis of a ReC_4Li Complex. Polyalkynyl homologs of the ReC_2M complexes in Scheme 1 were sought. The key precursor, ethynyl complex **1**, was prepared by a reaction sequence involving free ethyne.⁹ However, 1,3-butadiyne is explosive.¹⁷ Therefore, a similar sequence involving the readily available monosilyl derivative HC≡CC≡CSiMe₃¹⁸ was investigated.

Accordingly, the methyl complex ($\eta^5\text{-C}_5\text{Me}_5$) $\text{Re}(\text{NO})(\text{PPh}_3)$ -(CH₃) (**5**) was converted to the substitution-labile chlorobenzene complex $[(\eta^5\text{-C}_5\text{Me}_5)\text{Re}(\text{NO})(\text{PPh}_3)(\text{ClC}_6\text{H}_5)]^+\text{BF}_4^-$ (**6** $+\text{BF}_4^-$) at -45°C as reported earlier.¹⁹ As shown in Scheme 2, addition

(16) Parker, D. W.; Marsi, M. M.; Gladysz, J. A. *J. Organomet. Chem.* 1980, 194, C1.

(17) Brandsma, L. *Preparative Acetylenic Chemistry*, 2nd ed.; Elsevier: New York, 1988; p 179.

(18) This compound was prepared by reaction of LiC≡CC≡CSiMe₃ (Holmes, A. B.; Jennings-White, C. L. D.; Schulthess, A. H.; Akinde, B.; Walton, D. R. M. *J. Chem. Soc., Chem. Commun.* 1979, 840) and aqueous NH₄Cl: Zweifel, G.; Rajagopalan, S. *J. Am. Chem. Soc.* 1985, 107, 700.

(19) Peng, T.-S.; Winter, C. H.; Gladysz, J. A. *Inorg. Chem.* 1994, 33, 2534.

of excess $\text{HC}\equiv\text{CC}\equiv\text{CSiMe}_3$ gave two isomers of the formula $[(\eta^5\text{-C}_5\text{Me}_5)\text{Re}(\text{NO})(\text{PPh}_3)(\text{HC}\equiv\text{CC}\equiv\text{CSiMe}_3)]^+\text{BF}_4^-$ (7^+BF_4^-) in 95% yield (79–67:21–33). Both involved coordination of the $\text{C}\equiv\text{CH}$ linkage, as evidenced by downfield $\equiv\text{CH}$ ^1H NMR signals (δ 7.09, 8.24). Thus, they were assigned as rotamers about the $\text{Re}-(\text{C}\equiv\text{C})$ axis, as found for related adducts of unsymmetrical alkynes.^{9,20,21}

Reaction of 7^+BF_4^- and $t\text{-BuOK}$ gave the silylated 1,3-butadiynyl complex $(\eta^5\text{-C}_5\text{Me}_5)\text{Re}(\text{NO})(\text{PPh}_3)(\text{C}\equiv\text{CC}\equiv\text{CSiMe}_3)$ (**8**) in 96% yield after workup.²² Deprotection with $\text{K}_2\text{CO}_3/\text{MeOH}$ gave the 1,3-butadiynyl complex $(\eta^5\text{-C}_5\text{Me}_5)\text{Re}(\text{NO})(\text{PPh}_3)(\text{C}\equiv\text{CC}\equiv\text{CH})$ (**9**) in 84% yield.²³ Complex **9** melted without decomposition at 105–108 °C, did not deteriorate after 1 day in air, and could be stored under argon at 0 °C for months. However, **9** showed variable stability in solution, and was much more labile than **8**.

Many spectroscopic properties of **8** and **9** were similar to those of the lower alkynyl homologs.⁹ However, the IR ν_{NO} values were 7–20 cm^{-1} greater, and two $\nu_{\text{C}\equiv\text{C}}$ bands were present. These were of comparable frequency and intensity with **8** (2118–2119 m, 2097–2098 m), but quite different frequency and intensity with **9** (2115–2113 s, 1975 w; ranges reflect values in different media). Also, the $\equiv\text{CH}$ ^1H NMR signal and most $\text{C}\equiv\text{C}$ ^{13}C NMR signals were further upfield than in alkynyl homologs. Interestingly, the $\text{ReC}\equiv\text{CC}$ resonances gave detectable phosphorus couplings, whereas the $\text{ReC}\equiv\text{C}$ resonances did not.

Next, **9** and $n\text{-BuLi}$ (1.1–1.5 equiv) were combined in THF at –80 °C. A ^{31}P NMR monitored reaction showed signals at 21.3 and 21.0 ppm (70:30). The latter is very close to that of **9** in THF (21.0 ppm). However, ^{31}P NMR chemical shifts of $\text{ReC}\equiv\text{CC}\equiv\text{CX}$ species are much less sensitive to the nature of X than $\text{ReC}\equiv\text{CX}$ species. The signals appeared to coalesce upon warming, giving one sharp peak at 10–20 °C (21.0 ppm). Subsequent additions of MeI at either –80 °C or room temperature gave the 1,3-pentadiynyl complex $(\eta^5\text{-C}_5\text{Me}_5)\text{Re}(\text{NO})(\text{PPh}_3)(\text{C}\equiv\text{CC}\equiv\text{CMe})$ (**11**; 20.9 ppm) in ≥95% yields by NMR and IR, and 85% isolated yield. This indicates the formation of the ReC_4Li complex $(\eta^5\text{-C}_5\text{Me}_5)\text{Re}(\text{NO})(\text{PPh}_3)(\text{C}\equiv\text{CC}\equiv\text{CLi})$ (**10**), possibly as a mixture of aggregates.

The generation of **10** could be more effectively monitored by IR. The weaker $\nu_{\text{C}\equiv\text{C}}$ band of **9** (1975 cm^{-1}) was replaced by an absorption of comparable intensity (2081 cm^{-1}). No higher frequency band was observed. Additional $n\text{-BuLi}$ could be added in cases of incomplete conversion. Crude **10** could be isolated as an orange powder by workup at –10 °C. IR spectra of some samples showed small amounts of **9**. Complex **10** persisted for hours in THF at room temperature, as assayed by methylation to **11**.

3. Syntheses of ReC_4M Complexes. As shown in Scheme 3, *trans*- $\text{Pd}(\text{PEt}_3)_2(\text{Cl})_2$ was added to **10** in THF at –80 °C. In the case of a 1:2 stoichiometry, workup gave the dark red, air stable $\text{ReC}_4\text{PdC}_4\text{Re}$ complex *trans*-($\eta^5\text{-C}_5\text{Me}_5$) $\text{Re}(\text{NO})(\text{PPh}_3)(\text{C}\equiv\text{CC}\equiv\text{C})\text{Pd}(\text{PEt}_3)_2(\text{C}\equiv\text{CC}\equiv\text{C})(\text{Ph}_3\text{P})(\text{ON})\text{Re}(\eta^5\text{-C}_5\text{Me}_5)$ (**12**)

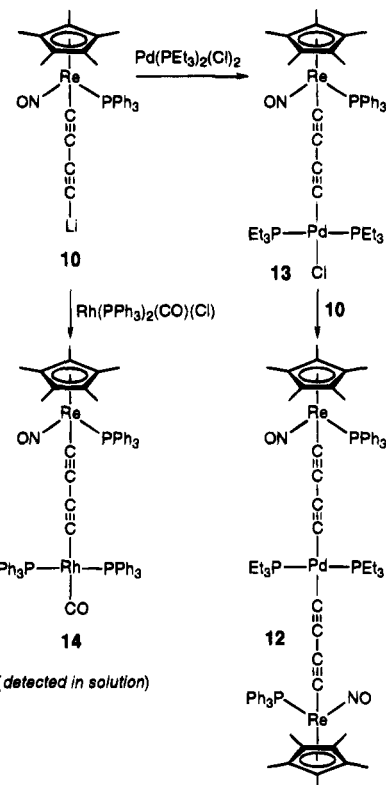
(20) Kowalczyk, J. J.; Arif, A. M.; Gladysz, J. A. *Organometallics* 1991, 10, 1079.

(21) The $\text{Re}-(\text{C}\equiv\text{C})$ conformations and NMR properties of such alkyne complexes have been analyzed in detail.^{9,20} The J_{CP} and J_{HP} values associated with the $\text{C}\equiv\text{CH}$ NMR signals of 7^+BF_4^- show that in the major isomer, the smaller $\equiv\text{CH}$ moiety is *syn* to the bulky PPh_3 ligand, and the larger $\equiv\text{CC}\equiv\text{CSiMe}_3$ moiety is *anti*.

(22) Reactions of metal halides and $\text{LiC}\equiv\text{CC}\equiv\text{CSiMe}_3$, or related nucleophiles can give similar species.^{6b,h} However, the rhodium halides $(\eta^5\text{-C}_5\text{Me}_5)\text{Rh}(\text{NO})(\text{PPh}_3)(\text{X})$ are synthesized from methyl complex **5**. Thus, analogous approaches to **8** would entail the same number of steps as that in Scheme 2.

(23) Eastmond, R.; Johnson, T. R.; Walton, D. R. M. *J. Organomet. Chem.* 1973, 50, 87.

Scheme 3. Syntheses of ReC_4M and $\text{ReC}_4\text{MC}_4\text{Re}$ Complexes



in 73% yield. Since **12** has two rhodium stereocenters, *meso* and *dl* diastereomers are possible. However, only a single set of NMR signals was detected. Diastereomers of related ReC_6Re and ReC_8Re complexes also give a single set of NMR signals.^{11c} Thus, the stereocenters are likely too far apart to afford diastereomers with detectable spectroscopic differences.

An analogous reaction was conducted with a 1:1 stoichiometry. Workup gave a 24:18:58 mixture of *trans*- $\text{Pd}(\text{PEt}_3)_2(\text{Cl})_2$, **12**, and a new compound (**13**), as assayed by ^{31}P NMR. Several reprecipitations gave a pure sample of the latter, which spectroscopic data showed to be the expected ReC_4Pd complex *trans*-($\eta^5\text{-C}_5\text{Me}_5$) $\text{Re}(\text{NO})(\text{PPh}_3)(\text{C}\equiv\text{CC}\equiv\text{C})\text{Pd}(\text{PEt}_3)_2(\text{Cl})$. A similar reaction was conducted with a 2:1 stoichiometry and inverse addition. Workup gave a 50:50 mixture of *trans*- $\text{Pd}(\text{PEt}_3)_2(\text{Cl})_2$ and **13** (>95%). One reprecipitation yielded a 4:96 mixture.

Complexes **12** and **13** were stable for days in air as solids, and displayed similar NMR properties. Most $\text{C}\equiv\text{C}$ ^{13}C NMR signals were further upfield than in the ReC_2Pd complex **3**. The IR ν_{NO} values were 12–14 cm^{-1} greater than that of **3**. Two IR $\nu_{\text{C}\equiv\text{C}}$ bands were detected for **12** (2114 w, 1984–1988 w), but only one for **13** (1988 w). Raman spectra showed two $\nu_{\text{C}\equiv\text{C}}$ bands for each (**12/13** 2111/2128, 2090/2093 cm^{-1}). Interestingly, mass spectra of **12**, **13**, and **3** exhibited ions of formal composition $(\eta^5\text{-C}_5\text{H}_5)\text{Re}(\text{NO})(\text{PPh}_3)(\text{C}_x\text{PEt}_3)_x^+$ ($x = 2$ or 4), indicating scission of the $\equiv\text{C}\text{–Pd}$ linkage. The UV–visible spectra of **12** and **3** were similar, with three shoulders (268, 314–308, 390–388 nm) on an intense absorption associated with the PPh_3 ligand (234 nm).

Similar reactions of *trans*- $\text{Rh}(\text{PPh}_3)_2(\text{CO})(\text{Cl})$ and **10** were attempted (Scheme 3). NMR experiments showed that the former was consumed much more slowly than in the reaction with ReC_2Li complex **2** (–80 °C for 1 h, then room temperature: 50% conversion, 24 h vs >98% conversion, 3 h). In this context, terminal 1,3-dynes are more acidic than analogous terminal alkynes.²³ Thus, **10** would be expected to be a weaker

Table 1. Summary of Crystallographic Data for *trans*-(η^5 -C₅(CH₃)₅)Re(NO)(PPh₃)(C≡C)Pd(PEt₃)₂(Cl) (3)

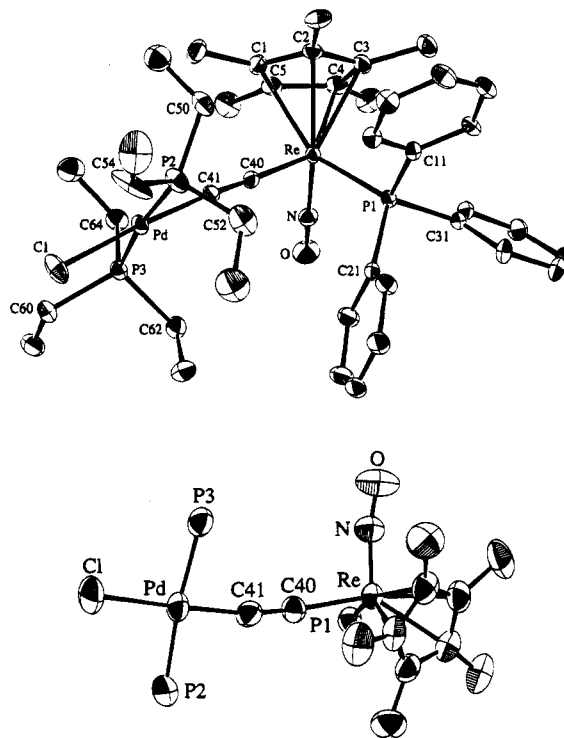
molecular formula	C ₄₂ H ₆₀ ClNOP ₃ PdRe
molecular wt	1015.928
cryst system	monoclinic
space group	P2 ₁ /n (non-standard setting of No. 14 P2 ₁ /c)
temp of collection, °C	16
cell dimens	
a, Å	16.304(4)
b, Å	14.861(3)
c, Å	18.457(6)
β , deg	101.09(2)
V, Å ³	4388(2)
Z	4
d_{calc} , g/cm ³	1.537
cryst dimens, mm	0.21 × 0.21 × 0.18
diffractometer	CAD4
radiation, Å	Mo K α (0.70930)
data collection method	θ -2 θ
scan speed, deg/min	variable (3–8)
no. of reflcns measured	8971
range/indices (h, k, l)	0.19, 0.17, -21.21
scan range	0.80 + 0.34 tan θ
2 θ limit, deg	2.0–50.0
standard reflcn check	1 X-ray h
total no. of unique data	7711
obsd data, $I > 3\sigma(I)$	4998
abs coeff, cm ⁻¹	33.98
min transmission, %	89.46
max transmission, %	99.96
no. of variables	451
goodness of fit	0.8962
$R = \sum F_O - F_C / \sum F_O $	0.0306
$R_w = [\sum w(F_O - F_C)^2 / \sum w F_O ^2]^{1/2}$	0.0329
$\Delta/\sigma(\text{max})$	0.010
$\Delta\rho(\text{max})$, e/Å ³	0.836

base and nucleophile than **2**—a trend that has been observed in another study.^{10d,13} Mass, IR, and ³¹P spectra of the crude product (Experimental Section) clearly showed that the ReC₄-Rh complex *trans*-(η^5 -C₅Me₅)Re(NO)(PPh₃)(C≡CC≡C)Rh-(PPh₃)₂(CO) (**14**) was the dominant component. However, purification attempts were unsuccessful.

In contrast to the facile condensation of the ReC₄Li and ReC₄-PdCl complexes **10** and **13** in Scheme 3, the ReC₂Li and ReC₂-PdCl complexes **2** and **3** did not react, even at room temperature. Since **2** is a stronger nucleophile than **10**, this must be due to the greater steric congestion that would be present in the target ReC₂PdC₂Re adduct.

4. Structural and Dynamic Properties. In order to confirm the assignment made above, the crystal structure of **3** was determined as outlined in Table 1 and the Experimental Section. Selected bond lengths and angles are given in Table 2. Two views are shown in Figure 1. The bulky nature of the ligands on each metal is apparent. There are no van der Waals contacts between the two metal fragments, as verified on a stereoscopic screen. However, rotation about any bond in the ReC≡CPd linkage generates modest van der Waals contacts.

The Re—C≡C and C≡C—Pd bond angles in **3** (173.2(9), 169.5(9)°) differ only moderately from 180°. However, they constitute the greatest distortions found to date in sp carbon chains linking the rhenium moiety (η^5 -C₅Me₅)Re(NO)(PPh₃) and a second metal fragment.^{10b,11a} The nitrosyl ligand is also bent more than usual (\angle Re—N—O 167.1(8)°). The bottom view in Figure 1 emphasizes these features, which are likely steric in origin. The Re—C and C≡C bond lengths (2.079(9), 1.21(1) Å) are close to those in the ReC₄Re complex^{11a} (η^5 -C₅Me₅)Re(NO)(PPh₃)(C≡CC≡C)(Ph₃P)(ON)Re(η^5 -C₅Me₅) (**15**;

**Figure 1.** Full (top) and partial (bottom) views of the molecular structure of **3**.**Table 2.** Key Bond Lengths (Å) and Bond Angles (deg) in **3**

Re—P1	2.359(3)	P2—C50	1.80(1)
Re—N	1.750(9)	P2—C52	1.82(2)
N—O	1.21(1)	P2—C54	1.77(2)
C40—C41	1.21(1)	P3—C60	1.82(1)
Re—C40	2.079(9)	P3—C62	1.82(1)
Pd—C41	1.967(9)	P3—C64	1.82(1)
Pd—Cl	2.358(3)	Re—C1	2.32(1)
Pd—P2	2.285(4)	Re—C2	2.29(1)
Pd—P3	2.295(3)	Re—C3	2.31(1)
P1—C11	1.81(1)	Re—C4	2.31(1)
P1—C21	1.84(1)	Re—C5	2.32(1)
P1—C31	1.83(1)		
P1—Re—N	93.8(3)	P2—Pd—P3	170.7(1)
Re—N—O	167.1(8)	Re—P1—C11	113.9(4)
P1—Re—C40	87.1(3)	Re—P1—C21	118.4(3)
N—Re—C40	100.5(4)	Re—P1—C31	115.7(3)
Re—C40—C41	173.2(9)	Pd—P2—C50	116.5(4)
Pd—C41—C40	169.5(9)	Pd—P2—C52	110.5(6)
P2—Pd—C41	87.0(3)	Pd—P2—C54	117(2)
P3—Pd—C41	84.7(3)	Pd—P3—C60	115.5(5)
Cl—Pd—C41	176.1(3)	Pd—P3—C62	109.9(4)
Cl—Pd—P2	94.7(1)	Pd—P3—C64	115.3(4)
Cl—Pd—P3	93.5(2)		

2.037(5), 1.202(7) Å). Similar Re—C, C≡C, and C—Pd bond lengths are found in other ReC≡C²⁴ and C≡CPd²⁵ species.

As is obvious from Figure 1, the *trans* phosphines of **3** and **4** are inequivalent in any static structure. Accordingly, low-

(24) Typical Re—C/C≡C bond lengths (Å): (a) 2.066(7)/1.19(1); Senn, D. R.; Wong, A.; Patton, A. T.; Marsi, M.; Strouse, C. E.; Gladysz, J. A. *J. Am. Chem. Soc.* **1988**, *110*, 6096. (b) 2.01(2)/1.19(3); Heidrich, J.; Steimann, M.; Appel, M.; Beck, W.; Phillips, J. R.; Trogler, W. C. *Organometallics* **1990**, *9*, 1296.

(25) Typical Pd—C/C≡C bond lengths (Å): (a) 1.939(8)/1.200(12); Onitsuka, K.; Ogawa, H.; Joh, T.; Takahashi, S.; Yamamoto, Y.; Yamazaki, H. *J. Chem. Soc., Dalton Trans.* **1991**, 1531. (b) 1.945(4)/1.193(6); de Graaf, W.; Harder, S.; Boersma, J.; van Koten, G.; Kanters, J. A. *J. Organomet. Chem.* **1988**, *358*, 545. (c) 1.974(6)/1.16(1); van der Voort, E.; Spek, A. L.; de Graaf, W. *Acta Crystallogr.* **1987**, *C43*, 2311. (d) 1.952(7)/1.20(1); Behrens, U.; Hoffmann, K. *J. Organomet. Chem.* **1977**, *129*, 273. (e) 2.03(2)–2.04(2)/1.20(2)–1.21(3); Yasuda, T.; Kai, Y.; Yasuoka, N.; Kasai, N. *Bull. Chem. Soc. Jpn.* **1977**, *50*, 2888.

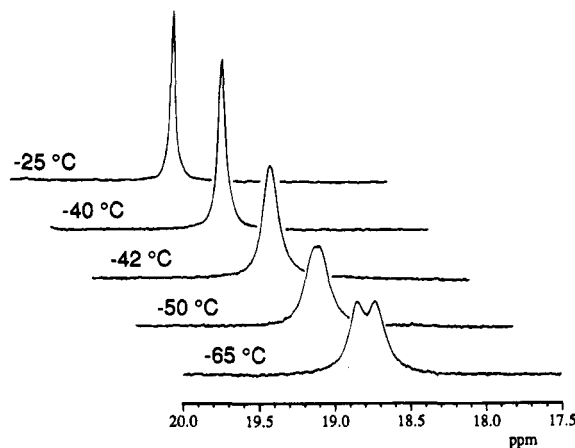


Figure 2. Variable-temperature $^{31}\text{P}\{^1\text{H}\}$ NMR spectra of **3** (THF- d_8 , PEt₃ region).

temperature ^{31}P NMR spectra showed two signals (**3**, THF- d_8 , -60 °C: 17.2/17.0 ppm; $\Delta\nu$ 20.4 Hz; **4**, CD₂Cl₂, -80 °C: 28.5/23.1 ppm; $\Delta\nu$ 555.6 Hz). These coalesced at -42 and -26 °C, respectively, giving $\Delta G^\ddagger(T_c)$ values of 11.7 ± 0.2 and 10.9 ± 0.2 kcal/mol for the processes that render the phosphines equivalent.²⁶ Representative spectra are shown in Figure 2.

We suggest that these phenomena arise from restricted rotation about the ReC≡CM linkages. A 180° rotation about any bond will exchange the *trans* phosphines, but generate van der Waals contacts as noted above. Importantly, the ReC≡CC≡CPd species **12** and **13** do not show similar behavior or line broadening (^{31}P and ^1H NMR, CD₂Cl₂, -80 °C). Also, rhodium coupling is maintained above T_c in **4** ($J_{\text{PRh}} = 143$ Hz). Hence, exchange mechanisms that entail phosphine dissociation can be excluded. The observation of rotational barriers involving alkyne substituents appears to be extremely rare.²⁷

Curiously, the phosphorus–carbon bonds of the *trans* PEt₃ ligands in **3** are essentially eclipsed (Figure 1). The PMe₃ ligands in the Pt₂C₂Pt complex *trans,trans*-(I)(Me₃P)₂Pt(C≡C)-Pt(PMe₃)₂(I) exhibit an analogous geometry in the solid state.²⁸ Many palladium complexes with *trans* PEt₃ ligands have been crystallographically characterized. Selected examples have been viewed stereoscopically. Some share this feature,^{25e} but the majority examined do not.^{25a,d}

5. Oxidations. We sought to generate some of the preceding complexes in different oxidation states. For example, as sketched in Scheme 4, loss of one electron from the ReC₂Pd complex **3** would give a radical cation **3⁺** that could be rhenium centered (**A**), palladium centered (**B**), or delocalized.²⁹ Loss of a second electron would generate a dication **3²⁺** that could be paramagnetic (**C**) or diamagnetic (**D**). The ReC₄Re complex **15** can be oxidized to the radical cation **15⁺** and diamagnetic dication **15²⁺**, both of which are isolable.¹¹ As shown in Scheme 5 (bottom), the former is delocalized. This is evidenced by an undecet ESR signal diagnostic of two equivalent rhenium nuclei, as opposed to the sextet commonly found for monorhenium radicals ($I = 5/2$ and virtually identical magnetic moments for both major isotopes). Similar FeC₄Fe complexes have been reported by Lapinte.^{6g,i}

Thus, cyclic voltammograms of the ReC_xPd complexes **3**, **12**, and **13** were acquired in CH₂Cl₂ as described in the

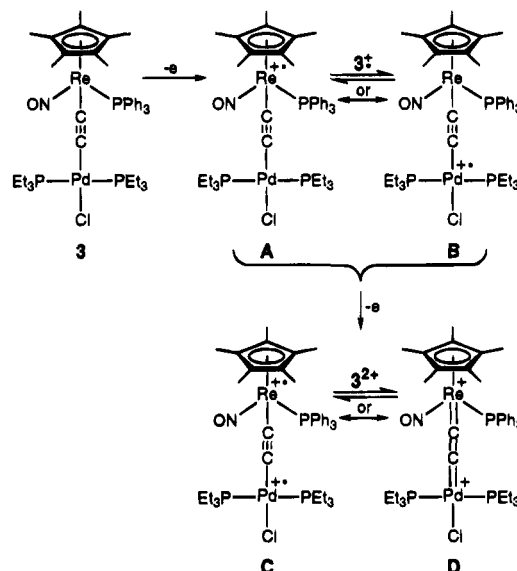
(26) Sandström, J. *Dynamic NMR Spectroscopy*; Academic Press: New York, 1982; Chapter 7.

(27) Mew, P. K. T.; Vögtle, F. *Angew. Chem., Int. Ed. Engl.* **1979**, *18*, 159.

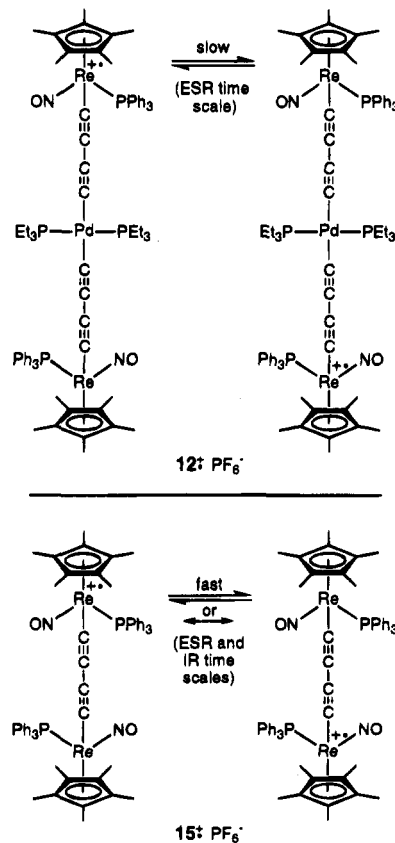
(28) Ogawa, H.; Onitsuka, K.; Joh, T.; Takahashi, S.; Yamamoto, Y.; Yamazaki, H. *Organometallics* **1988**, *7*, 2257.

(29) (a) Creutz, C. *Prog. Inorg. Chem.* **1983**, *30*, 1. (b) Sponsler, M. B. *Organometallics* **1995**, *14*, 1920 and references therein.

Scheme 4. Some Possible Oxidation Products of **3**



Scheme 5. Electron Delocalization in Dirhenium Radical Cations



Experimental Section. For reference, voltammograms of the methyl complex **5**, propynyl complex ($\eta^5\text{-C}_5\text{Me}_5$)Re(NO)(PPh₃)-(C≡CCH₃) (**16**),⁹ 1,3-pentadiynyl complex **11**, and bis(phenyl-ethynyl)palladium complex *trans*-Pd(PEt₃)₂(C≡CPh)₂ (**17**)³⁰ were recorded under identical conditions. Complexes **3**, **12**, and **13** gave chemically reversible one-electron oxidations, and irreversible second oxidations, as illustrated by the representative traces in Figure 3. The methyl complex **5** also gave a reversible one-electron oxidation. However, the monometallic alkynyl

(30) (a) Calvin, G.; Coates, G. E. *J. Chem. Soc.* **1960**, 2008. (b) Davey, A. P.; Cardin, D. J.; Byrne, H. J.; Blau, W. In *Organic Molecules of Nonlinear Optics and Photonics*; Messier, J., Kajzar, F., Prasad, P., Eds.; Kluwer: Boston, 1991; pp 391–402.

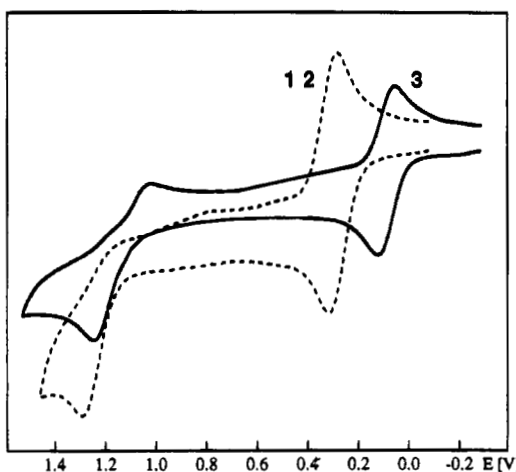


Figure 3. Cyclic voltammograms of **3** and **12** recorded in CH_2Cl_2 at 100 mV/s as described in the Experimental Section (E° (ferrocene) = 0.56 V).

Table 3. Cyclic Voltammetry Data^a

compd ^b	$E_{p,a}$ [V]	$E_{p,c}$ [V]	E° [V]	ΔE [mV]	$E'_{p,a}$ [V] ^c
$[\text{Re}^*]\text{CH}_3$ (5)	0.32	0.25	0.29	70	
$[\text{Re}^*]\text{C}\equiv\text{CCH}_3$ (16)	0.40				
$[\text{Re}^*]\text{C}\equiv\text{CC}\equiv\text{CCH}_3$ (11)	0.52				
$[\text{Re}^*]\text{C}\equiv\text{C}[\text{Pd}]\text{Cl}$ (3)	0.12	0.05	0.08	70	1.25
$[\text{Re}^*]\text{C}\equiv\text{CC}\equiv\text{C}[\text{Pd}]\text{Cl}$ (13)	0.35	0.28	0.32	70	1.29
$[\text{Re}^*]\text{C}\equiv\text{CC}\equiv\text{C}[\text{Pd}]\text{C}\equiv\text{CC}\equiv\text{C}[\text{Re}^*]$ (12)	0.36	0.28	0.32	80	1.29
$[\text{Re}^*]\text{C}\equiv\text{CC}\equiv\text{C}[\text{Re}^*]$ (15) ^d	0.15	0.06	0.11	90	0.68
$\text{PhC}\equiv\text{C}[\text{Pd}]\text{C}\equiv\text{CPh}$ (17)	1.48				

^a Recorded in CH_2Cl_2 at ambient temperature at 100 mV/s as detailed in the Experimental Section. ^b $[\text{Re}^*] = (\eta^5\text{-C}_5\text{Me}_5)\text{Re}(\text{NO})(\text{PPh}_3)$, $[\text{Pd}] = \text{Pd}(\text{PPh}_3)_2$. ^c For a second oxidation (irreversible for **3**, **12**, and **13**). ^d Data from ref 11c.

complexes **16**, **11**, and **17** were irreversibly oxidized. The palladium complex **17** was ca. 1.0 V more difficult to oxidize than any other compound. Data are summarized in Table 3, and analyzed further in the Discussion section.

These results indicate that the ReC_xPd dications **3**²⁺, **12**²⁺, and **13**²⁺ rapidly decompose in CH_2Cl_2 at room temperature. However, the corresponding radical cations, and that derived from methyl complex **5**, are much more stable. Thus, preparative oxidations were attempted. First, **5** and Ag^+PF_6^- or $(\eta^5\text{-C}_5\text{H}_5)_2\text{Fe}^+\text{PF}_6^-$ (0.95 equiv) were combined in CH_2Cl_2 in ESR tubes at room temperature. The solutions turned brown, and spectra were immediately recorded. A representative trace is depicted in Figure 4 (top; $g = 2.110\text{--}2.121$; $A_{\text{iso},\text{Re}} = 195\text{--}190$ G). The sextet signal is consistent with a rhenium-centered radical such as **5**⁺ PF_6^- . After 1–12 h, significant decomposition had occurred, as evidenced by two overlapping sextets of approximately equal intensities (new signal, $g = 2.096$, $A_{\text{iso},\text{Re}} = 185$ G). Importantly, the $A_{\text{iso},\text{Re}}$ value for **5**⁺ PF_6^- was approximately twice that of **15**⁺ PF_6^- (98 G; $g = 2.018$),^{11b} in which the odd electron is delocalized onto two rheniums.

Next, **3** and **12** were analogously treated with $(\eta^5\text{-C}_5\text{H}_5)_2\text{Fe}^+\text{PF}_6^-$. ESR spectra of the resulting purple and blue-green solutions showed weak sextets, consistent with **3**⁺ PF_6^- and **12**⁺ PF_6^- (Figure 4, middle and bottom; $g = 2.070, 2.032$; $A_{\text{iso},\text{Re}} = 180, 140$ G). The signals vanished after 5–15 min. The multiplicities and $A_{\text{iso},\text{Re}}$ values indicate that the odd electrons are localized mainly on (one) rhenium. Hence, the $\text{C}\equiv\text{CC}\equiv\text{C}\text{PdC}\equiv\text{CC}\equiv\text{C}$ linkage in **12**⁺ PF_6^- does not allow electron delocalization between the rhenium termini, at least on the rapid time scale found with **15**⁺ PF_6^- (Scheme 5).

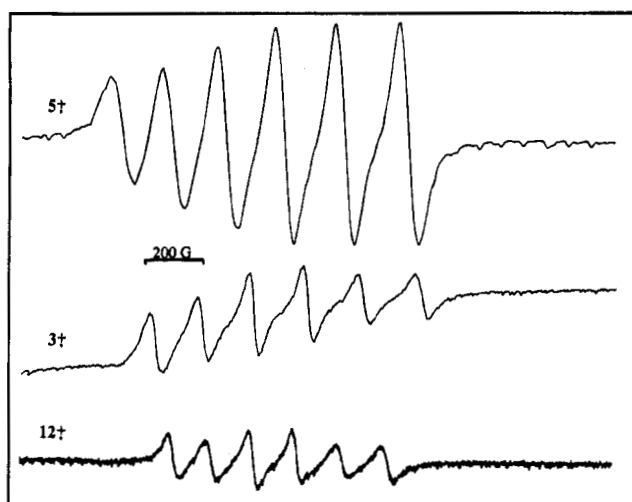
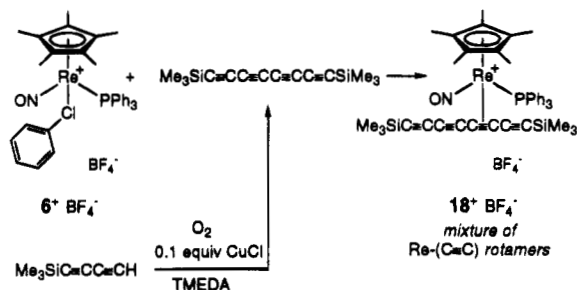


Figure 4. ESR spectra of radical cations **5**⁺ PF_6^- (top), **3**⁺ PF_6^- (middle), and **12**⁺ PF_6^- (bottom) in CH_2Cl_2 at ambient temperature.

Scheme 6. Synthesis and Complexation of Bis(trimethylsilyl)octa-1,3,5,7-tetrayne



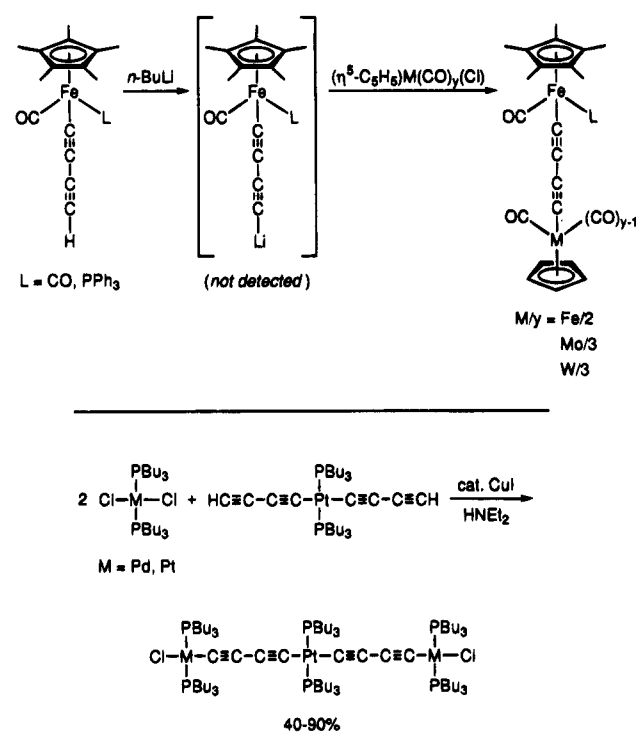
6. Extensions. We sought to adapt Scheme 2 to complexes with yet longer sp carbon chains. One obvious approach would involve terminal alkynes of the formula $\text{H}(\text{C}\equiv\text{C})_x\text{SiR}_3$. Although several compounds with $x \geq 3$ have been generated in solution, they are extremely labile and do not appear to have been isolated in pure form.³¹ Thus, as shown in Scheme 6, the chlorobenzene complex **6**⁺ BF_4^- and the known octatetrayne $\text{Me}_3\text{SiC}\equiv\text{CC}\equiv\text{CC}\equiv\text{CC}\equiv\text{CSiMe}_3$ ³² were reacted. Workup gave the π adduct $[(\eta^5\text{-C}_5\text{Me}_5)\text{Re}(\text{NO})(\text{PPh}_3)(\text{Me}_3\text{SiC}\equiv\text{CC}\equiv\text{CC}\equiv\text{C}\equiv\text{CSiMe}_3)]^+\text{BF}_4^-$ (**18**⁺ BF_4^-) in 48% yield. Only the internal $\text{CC}\equiv\text{CC}$ linkage was coordinated. Two $\text{Re}-(\text{C}\equiv\text{C})$ rotamers were present (60:40), as with **7**⁺ BF_4^- above.

Disappointingly, numerous efforts to convert **18**⁺ BF_4^- to a π complex with a $\equiv\text{CH}$ end group, or a σ 1,3,5,7-octatetraynyl species of the formula $(\eta^5\text{-C}_5\text{Me}_5)\text{Re}(\text{NO})(\text{PPh}_3)(\text{C}\equiv\text{CC}\equiv\text{C}\equiv\text{CC}\equiv\text{CX})$, were unsuccessful. These included reactions with MeOH, MeOH/K₂CO₃, MeLi, t-BuOK, and other reagents. In all cases, ³¹P NMR spectra showed many products. We had also hoped that thermolyses might extrude FSiMe_3 , but melting actually occurred without decomposition (78 °C). Perhaps the rhenium must migrate to a terminal $\text{SiC}\equiv\text{CC}$ linkage before a σ complex can form. Since the $\text{Re}-(\text{C}\equiv\text{C})$ rotamers can in principle interconvert by similar migrations, yet do not on NMR time scales, the activation barriers appear to be appreciable. Regardless, other strategies have been developed that allow access to compounds with higher sp carbon chains.¹²

(31) (a) Eastmond, R.; Johnson, T. R.; Walton, D. R. M. *Tetrahedron* **1972**, *28*, 4601. (b) Yamaguchi, M.; Park, H.-J.; Hirama, M.; Torisu, K.; Nakamura, S.; Minami, T.; Nishihara, H.; Hiraoka, T. *Bull. Chem. Soc. Jpn.* **1994**, *67*, 1717.

(32) (a) Walton, D. R. M.; Waugh, F. J. *Organomet. Chem.* **1972**, *37*, 45. (b) Since yields are a sensitive function of conditions, full details of our version of the original synthesis are given in this paper.

Scheme 7. Other Routes to MC_4Li and $MC_4M'C_4M$ Species^{6a,b}



Discussion

The reactions in Schemes 1 and 3 establish that the $\text{ReC}\equiv\text{CLi}$ and $\text{ReC}\equiv\text{CC}\equiv\text{CLi}$ species **2** and **10** are versatile precursors to ReC_2M , ReC_4M , and $\text{ReC}_4\text{MC}_4\text{Re}$ complexes. Furthermore, Wong has reported that reactions of iron 1,3-butadiynyl complexes ($\eta^5\text{-C}_5\text{H}_5\text{Fe}(\text{CO})(\text{L})(\text{C}\equiv\text{CC}\equiv\text{CH})$) and $n\text{-BuLi}$, followed by iron, molybdenum, or tungsten chlorides, give FeC_4M complexes as shown in Scheme 7.^{6b} Although spectroscopic monitoring was not attempted, these transformations were logically interpreted as involving $\text{FeC}\equiv\text{CC}\equiv\text{CLi}$ species. Several other 1,3-butadiynyl complexes have been reported,^{6a,h} and in our opinion can likely be deprotonated similarly.³³

In a parallel effort, we have found that **2** and **10** can add to carbon monoxide ligands of metal carbonyl complexes.^{10b-d,13} The adducts can be elaborated to Fischer carbene complexes and then ReC_3M and ReC_5M complexes. This constitutes the only route available to such compounds at present. However, one other synthesis of a $\text{MC}_4\text{M}'\text{C}_4\text{M}$ complex has been described. As shown in Scheme 7 (bottom), Hagiwara was able to condense both termini of a bis(1,3-butadiynyl)platinum complex with palladium and platinum dichlorides.^{6a} Related polymers were also characterized.

The ReC_2Pd and $\text{ReC}_4\text{PdC}_4\text{Re}$ complexes **3** and **12** are easily oxidized to the labile radical cations 3^+PF_6^- and 12^+PF_6^- . To our knowledge, these represent the first radical cations derived from *heterobimetallic* $\text{MC}_x\text{M}'$ complexes. In such compounds, one metal terminus will usually be more basic or electron rich than the other, and better able to stabilize a positive charge. The $E_{\text{p},\text{a}}$ values for the monorhenium and monopalladium complexes **16** and **17** (Table 3) suggest that for the

(33) Some syntheses of C_2 complexes may involve transient $\text{MC}\equiv\text{CLi}$ or related species: (a) Ustyuk, N. A.; Vinogradova, V. N.; Krautsov, D. N.; Oprunenko, Yu. F.; Piven, V. A. *Metallorg. Khim.* **1988**, *1*, 884. *Chem. Abstr.* **1989**, *111*, 233074c. (b) Müller, T. E.; Choi, S. W.-K.; Mingos, D. M. P.; Murphy, D.; Williams, D. J.; Yam, V. W.-W. *J. Organomet. Chem.* **1994**, *484*, 209. (c) Gamasa, M. P.; Gimeno, J.; Godefroy, I.; Lastra, E.; Martin-Vaca, B. M.; Garcia-Granda, S.; Gutierrez-Rodriguez, A. *J. Chem. Soc., Dalton Trans.* **1995**, 1901.

equilibrium $16^+ + 17 \rightleftharpoons 16 + 17^+$, the rhenium radical cation should be favored by ca. 16 orders of magnitude. Thus, the rhenium in bimetallic complexes **3**, **12**, and **13** should be much more readily oxidized than palladium, and the localized nature of the resulting radical cations (e.g., structure A, Scheme 4) is not surprising.

Furthermore, the odd electron in 12^+PF_6^- is not rapidly delocalized between the symmetry-related rhenium termini. Apparently, the nine-atom $\text{C}\equiv\text{CC}\equiv\text{CPdC}\equiv\text{CC}\equiv\text{C}$ assembly cannot efficiently relay charge, whereas the four-atom $\text{C}\equiv\text{CC}\equiv\text{C}$ moiety in the dirhenium radical cation 15^+PF_6^- can (Scheme 5).^{11b} Lapinte has isolated a related diiron radical cation in which the odd electron is similarly delocalized across a $\text{C}\equiv\text{CC}\equiv\text{C}$ moiety.^{6g-i} Investigations are in progress with other compounds that may help interpret these differences. However, at this time we believe that the palladium atom in 12^+PF_6^- provides the principal barrier to delocalization.

Table 3 shows that oxidation is thermodynamically more favorable for the ReC_2Pd complex **3** than the ReC_4Pd complexes **12** and **13** ($\Delta E^\circ = 0.23\text{--}0.24$ V). The ReC_2Me and ReC_4Me complexes **16** and **11** exhibit a similar trend ($\Delta E_{\text{p},\text{a}} = 0.12$ V). Also, the ReC_4Re complex **15** is more readily oxidized than ReC_6Re and ReC_8Re homologs.^{11c,12} Hence, oxidations appear to become thermodynamically less favorable as the sp carbon segments are lengthened. Since the HOMO energies of conjugated polyynes that have organic endgroups *increase* as unsaturation is extended, this trend at first seems counterintuitive.³⁴

However, the HOMOs of most transition metal complexes are predominantly metal centered.^{29b} This has been unequivocally established by photoelectron spectroscopy (PES) for many adducts of rhenium fragments ($\eta^5\text{-C}_5\text{R}_5\text{Re}(\text{NO})(\text{L})$,³⁵ and various alkynyl complexes.³⁶ PES spectra show that HOMO energies of polyynes $\text{H}(\text{C}\equiv\text{C})_n\text{H}$ ($n = 2\text{--}4$) are at least 1 eV lower.³⁴ Regardless, the iron 1,3-butadiynyl complex ($\eta^5\text{-C}_5\text{H}_5\text{Fe}(\text{CO})_2(\text{C}\equiv\text{CC}\equiv\text{CH})$) has a higher HOMO energy than the corresponding ethynyl complex³⁶ and should—in contrast to the trend with **16** and **11**—be more easily oxidized. Thus, electrochemical studies of additional compounds, as well as theoretical calculations, are in progress to help identify the many possible contributing factors.

In conclusion, based upon the successful results described above and elsewhere,^{6b,10b-d,13} $\text{MC}\equiv\text{CLi}$ and $\text{MC}\equiv\text{CC}\equiv\text{CLi}$ species are certain to see increasing use in the preparation of diverse types of C_x complexes. Furthermore, many interesting reactions can be envisioned for the new ReC_2M , ReC_4M , and $\text{ReC}_4\text{MC}_4\text{Re}$ compounds in Schemes 1–3. However, our primary objective at present is the synthesis of complexes with still longer C_x chains, some of which should aid understanding of unresolved issues noted above. Although the strategy represented by Scheme 6 did not prove fruitful, other routes to higher ($\eta^5\text{-C}_5\text{Me}_5\text{Re}(\text{NO})(\text{PPh}_3)(\text{C}\equiv\text{C})_x\text{Li}$ species and adducts thereof have been very successful, and will be communicated shortly.¹²

(34) Gleiter, R.; Schäfer, W. In *Supplement C2: The Chemistry of Triple-Bonded Functional Groups*; Patai, S., Ed.; Wiley: New York, 1994; pp 157–180.

(35) (a) Lichtenberger, D. L.; Rai-Chaudhuri, A. R.; Seidel, M. J.; Gladysz, J. A.; Agbossou, S. K.; Igau, A.; Winter, C. H. *Organometallics* **1991**, *10*, 1355. (b) Lichtenberger, D. L.; Gruhn, N. E.; Rai-Chaudhuri, A.; Renshaw, S. K.; Gladysz, J. A.; Seyler, J.; Igau, A. Submitted for publication.

(36) (a) Lichtenberger, D. L.; Renshaw, S. K.; Bullock, R. M. *J. Am. Chem. Soc.* **1993**, *115*, 3276. (b) Lichtenberger, D. L.; Renshaw, S. K.; Wong, A.; Tagge, C. D. *Organometallics* **1993**, *12*, 3522, and references therein.

Experimental Section

General Data. All reactions were carried out under inert atmospheres. NMR, IR, and UV-visible spectra were recorded on Varian XL-300, Mattson Polaris FT, and Hewlett Packard 8452A spectrometers, respectively.³⁷ Raman spectra were recorded on a Spex 1877E spectrometer using an argon laser (514.5 nm) and 1–2 s acquisition times. Mass spectra were obtained on a Finnigan MAT 95 high-resolution instrument. Microanalyses were conducted by Atlantic Microlab.

Solvents and reagents were purified as follows: C₆H₅Cl, distilled from P₂O₅; CH₂Cl₂, distilled from CaH₂; ether, THF, hexane, benzene, distilled from Na/benzophenone; CD₂Cl₂ and CDCl₃, vacuum transferred from CaH₂; C₆D₆ and THF-*d*₈, vacuum transferred from LiAlH₄; *n*-BuLi (Aldrich), standardized according to Kofron (Kofron, W. G.; Baclawski, L. M. *J. Org. Chem.* 1976, 41, 1879). Other reagents and solvents were used as received from commercial suppliers.

trans-(η⁵-C₅Me₅)Re(NO)(PPh₃)(C≡C)Pd(PEt₃)₂(Cl) (3). A Schlenk flask was charged with (η⁵-C₅Me₅)Re(NO)(PPh₃)(C≡CH) (1;⁹ 0.053 g, 0.083 mmol) and THF (5 mL) and cooled to –80 °C (acetone/CO₂). Then *n*-BuLi (2.2 M in hexane; 41 μL, 0.091 mmol) was added with stirring. After 1 h, the solution was added by cannula to a stirred –45 °C (CH₃CN/CO₂) solution of *trans*-Pd(PEt₃)₂(Cl)₂ (0.041 g, 0.099 mmol)¹⁴ in THF (5 mL). The cold bath was allowed to warm to room temperature. After 3 h, hexane (60 mL) was added. The suspension was passed through a medium-frit Kramer filter, and solvent was removed by oil pump vacuum. The residue was dissolved in hot hexane (80 mL). The solution was filtered and kept at room temperature for 14 h. Dark red microcrystals formed, which were collected by filtration and dried by oil pump vacuum to give 3 (0.052 g, 0.051 mmol, 66%), mp 147–150 °C dec. Calcd for C₄₂H₆₀ClNOP₃PdRe: C, 49.66; H, 5.95. Found: C, 49.51; H, 5.92. IR (CH₂Cl₂/KBr)³⁷ ν_{C≡C} 1989/1994 w, ν_{NO} 1622/1622 vs. Raman (CH₂Cl₂) ν_{C≡C} 1971. UV-vis (nm (ε, M^{−1} cm^{−1}), 2.0 × 10^{−5} M CH₂Cl₂) 234 (76000), 268 sh (35000), 314 sh (17000), 390 sh (4000). MS (positive FAB, 3-NBA/CH₂Cl₂)³⁸ 1016 (3⁺ + 1, 92%), 898 (3⁺ – PEt₃ + 1, 43%), 756 ((η⁵-C₅Me₅)-Re(NO)(PPh₃)(C₂PEt₃)⁺, 55%), 638 ((η⁵-C₅Me₅)Re(NO)(PPh₃)(C₂)⁺, 100%), 614 ((η⁵-C₅Me₅)Re(NO)(PPh₃)⁺, 20%); no other peaks above 310 of >20%.

NMR (C₆D₆):³⁷ ¹H 7.84–7.62 (m, 6H of 3C₆H₅), 7.22–6.87 (m, 9H of 3C₆H₅), 1.93 (m, 2P(CH₂CH₃)₃), 1.14 (virtual quint, *J*_{HH} = 8.0, 2P-(CH₂CH₃)₃), 1.69 (s, C₅(CH₃)₅); ¹³C{¹H} 137.1 (d, *J*_{CP} = 50.3, *i*-Ph), 134.6 (d, *J*_{CP} = 10.7, *o*-Ph), 129.7 (d, *J*_{CP} = 1.7, *p*-Ph), 128.0 (d, *J*_{CP} = 9.9, *m*-Ph), 116.2 (dt, *J*_{CPPh} = 1.5, *J*_{CPEt} = 17.5, ≡CPd), 111.7 (dt, *J*_{CPPh} = 15.1, *J*_{CPEt} = 4.3, ReC≡C), 99.7 (d, *J* = 1.9, C₅(CH₃)₅), 15.8 (virtual t, *J*_{CP} = 13.4, P(CH₂CH₃)₃), 10.2 (s, C₅(CH₃)₅), 8.7 (s, P(CH₂CH₃)₃); ³¹P{¹H} 22.7 (s, ReP), 17.7 (s, PdP).

trans-(η⁵-C₅Me₅)Re(NO)(PPh₃)(C≡C)Rh(PPh₃)₂(CO) (4). A Schlenk tube was charged with 1 (0.0638 g, 0.100 mmol) and THF (5 mL) and cooled to –80 °C. Then *n*-BuLi (2.46 M in hexane; 65 μL, 0.160 mmol) was added with stirring. After 1.5 h, a solution of *trans*-Rh(PPh₃)₂(CO)(Cl) (0.0760 g, 0.110 mmol)¹⁵ in THF (5 mL) was added by cannula. The cold bath was kept at –80 °C for 1 h, and then allowed to slowly warm to room temperature. After 3 h, solvent was removed by oil pump vacuum, and the residue was extracted with ether (2 × 10 mL). The extracts were passed through a medium-frit Kramer filter, concentrated to ca. 3 mL, and kept at –20 °C for 24 h. The dark red microcrystals were collected by filtration and dried by oil pump vacuum to give 4 (0.0928 g, 0.0718 mmol, 72%), mp 165–168 °C dec. Calcd for C₆H₆₀NO₂P₂ReRh: C, 62.23; H, 4.68; P, 7.19. Found: C, 61.80; H, 4.32; P, 7.09. IR (CH₂Cl₂/KBr)³⁷ ν_{C≡C} 2023/2017 w, ν_{CO} 1961/1961 vs, ν_{NO} 1629/1623. MS (positive FAB, tetraglyme/benzene)³⁸ 1293 (4⁺, 100%); no other peaks above 500 of >20%.

NMR (C₆D₆):³⁷ ¹H 8.21–8.15 (m, 12H of 9C₆H₅), 7.97–7.89 (m, 6H of 9C₆H₅), 7.09–6.98 (m, 18H of 9C₆H₅), 6.91–6.88 (m, 9H of 9C₆H₅), 1.28 (s, C₅(CH₃)₅); ¹³C{¹H} 192.9 (dt, *J*_{CRh} = 57.0, *J*_{CP} = 16.2, CO), 138.4 (d, *J*_{CP} = 47.3, *i*-RePPh), 134.8 (d, *J*_{CP} = 10.8, *o*-RePPh),

(37) All ¹H, ¹³C, and ³¹P NMR data are in δ, ppm, and ppm, respectively. All *J* values are in Hz. All IR and Raman data are in cm^{−1}, and values obtained in different media are separated by a slash (/).

(38) *m/z* for the most intense peak of isotope envelope; relative intensities are for the specified mass range.

129.5 (s, *p*-RePPh), 127.7 (d, *J*_{CP} = 9.7, *m*-RePPh), 137.3 (virtual t, *J*_{CP} = 20.9, *i*-RhPPh), 135.7 (virtual t, *J*_{CP} = 6.5, *o*-RhPPh), 129.4 (s, *p*-RhPPh), 128.1 (virtual t, *J*_{CP} = 4.8, *m*-RhPPh),³⁹ 153.4 (dt, *J*_{CRh} = 37.7, *J*_{CP} = 21.2, ≡CRh), 134.6 (d, *J*_{CP} = 10.5, ReC≡C), 99.7 (s, C₅(CH₃)₅), 9.7 (s, C₅(CH₃)₅); ³¹P{¹H} 21.3 (s, ReP), 27.8 (d, *J*_{PRh} = 143, RhP).

[(η⁵-C₅Me₅)Re(NO)(PPh₃)(HC≡CC≡CSiMe₃)]⁺ BF₄[−] (7⁺ BF₄[−]). A Schlenk tube was charged with (η⁵-C₅Me₅)Re(NO)(PPh₃)(CH₃) (5;⁴⁰ 0.194 g, 0.309 mmol) and C₆H₅Cl (5 mL) and cooled to –45 °C. Then HBF₄·OEt₂ (8.2 M in ether; 55 μL, 0.45 mmol) was added with stirring. After 10 min, HC≡CC≡CSiMe₃ (0.18 mL, 0.15 g, 1.2 mmol)¹⁸ was added, and the cold bath was removed. After 24 h, solvent was removed by oil pump vacuum, and CH₂Cl₂ (2 mL) was added. The mixture was filtered through a Celite pad (2 cm) and added dropwise to rapidly stirred hexane (50 mL). The tan powder was collected by filtration and dried by oil pump vacuum to give 7⁺ BF₄[−] (0.236 g, 0.287 mmol, 93%); 79–67.21–33 mixture of Re(C≡C) rotamers), mp 118–121 °C dec. Calcd for C₃₅H₄₀BF₄NOPReSi: C, 51.09; H, 4.91. Found: C, 50.61; H, 4.62. IR (CH₂Cl₂/KBr)³⁷ ν_{C≡C} 2139/2138 w, ν_{NO} 1706/1694 vs. MS (positive FAB, 3-NBA/CH₂Cl₂)³⁸ 736 (7⁺, 100%), 614 ((η⁵-C₅Me₅)Re(NO)(PPh₃)⁺, 28%); no other peaks above 225 of >20%.

NMR (major/minor Re–(C≡C) rotamer):^{21,37} ¹H (CD₂Cl₂) 7.79–7.50 (m, 6H of 3C₆H₅), 7.48–7.31 (m, 9H of 3C₆H₅), 7.09/8.24 (d, *J*_{HP} = 19.7/4.7, ≡CH syn/anti to PPh₃), 1.85/1.77 (s, C₅(CH₃)₅), 0.34/−0.37 (s, Si(CH₃)₃); ¹³C{¹H} (CD₂Cl₂) 134.0 (d, *J*_{CP} = 10.7, *o*-PPh), 133.3 (br s, *p*-PPh), 129.9 (br d, *J*_{CP} = 3.7, *m*-PPh),⁴¹ 114.9/113.2 (s, C≡CSi), 110.3/109.9 (s, C₅(CH₃)₅), 92.1/92.9 (d, *J*_{CP} = 3.6/7.0, HC≡C), 96.6/108.0 (d, *J*_{CP} = 18.0/2.4, HC≡C), 95.2/110.4 (s, C≡CSi), 9.65 (s, C₅(CH₃)₅), −0.51/−0.98 (s, Si(CH₃)₃); ³¹P{¹H} (C₆D₆) 17.6/21.2 (s).

(η⁵-C₅Me₅)Re(NO)(PPh₃)(C≡CC≡CSiMe₃) (8). A Schlenk flask was charged with 7⁺ BF₄[−] (0.125 g, 0.152 mmol) and *t*-BuOK (0.021 g, 0.18 mmol) and cooled to –80 °C. Then THF (8 mL) was added with stirring. After 10 min, the cold bath was removed. After 1 h, solvent was removed by oil pump vacuum. The residue was extracted with benzene (3 × 5 mL). The extract was filtered through a Celite pad (2 cm), and solvent was removed by oil pump vacuum. The residue was dissolved in a minimum of CH₂Cl₂ and hexane (40 mL) was added. Solvent was removed by oil pump vacuum to give 8 as an orange powder (0.107 g, 0.146 mmol, 96%), mp 105–108 °C dec. Calcd for C₃₅H₃₉NOPReSi: C, 57.20; H, 5.35. Found: C, 57.36; H, 5.40. IR (CH₂Cl₂/KBr)³⁷ ν_{C≡C} 2118/2119 m, 2098/2097 m, ν_{NO} 1653/1648 vs. MS (EI, 30 eV)³⁸ 735 (8⁺, 100%); no other peaks >10%.

NMR (C₆D₆):³⁷ ¹H NMR 7.75–7.63 (m, 6H of 3C₆H₅), 7.04–6.95 (m, 9H of 3C₆H₅), 1.55 (s, C₅(CH₃)₅), 0.17 (s, Si(CH₃)₃); ¹³C{¹H} 135.3 (d, *J*_{CP} = 51.6, *i*-PPh), 134.3 (d, *J*_{CP} = 10.7, *o*-PPh), 130.1 (d, *J*_{CP} = 2.3, *p*-PPh), 128.4 (d, *J*_{CP} = 10.1, *m*-PPh), 112.3 (s, ReC≡C),⁴² 105.8 (d, *J*_{CP} = 15.9, ReC≡C), 100.6 (s, C₅(CH₃)₅), 93.5 (d, *J*_{CP} = 2.7, C≡CSi),⁴² 80.6 (s, C≡CSi), 10.0 (s, C₅(CH₃)₅), 0.91 (s, Si(CH₃)₃); ³¹P{¹H} 21.1 (s).

(η⁵-C₅Me₅)Re(NO)(PPh₃)(C≡CC≡CH) (9). A Schlenk flask was charged with 8 (0.104 g, 0.141 mmol), K₂CO₃ (2–4 mol %), and MeOH (20 mL). The mixture was stirred vigorously. After 8 h, solvent was removed by oil pump vacuum. The residue was extracted with THF (2 × 5 mL). The extract was filtered through a silica gel pad (3 cm),

(39) This resonance was partially obscured by C₆D₆, and was assigned from a spectrum recorded in CD₂Cl₂ (127.9 ppm, virtual t, *J*_{CP} = 4.8 Hz).

(40) Patton, A. T.; Strouse, C. E.; Knobler, C. B.; Gladysz, J. A. *J. Am. Chem. Soc.* 1983, 105, 5804.

(41) Complex PPh₃ ¹³C resonance patterns were observed, presumably due to restricted rotation about the Re–P and/or P–C bonds.

(42) Proton-coupled ¹³C NMR spectra, including literature data for HC≡CC≡CH (¹*J*_{CH} = 260.0–259.1; ²*J*_{CH} = 53.0–51.9; ³*J*_{CH} = 6.7–6.5; ⁴*J*_{CH} = 0.5–0.4),⁴³ allow PReC≡CC≡C resonances to be assigned and establish the trend ²*J*_{CP} > ⁴*J*_{CP} > ³*J*_{CP}. Data (THF-*d*₈): 9, 110.9 (d, ³*J*_{CH} = 5.3, ReC≡C), 101.4 (d, ²*J*_{CP} = 15.8, ReC≡C), 72.5 (dd, ⁴*J*_{CP} = 2.7, ²*J*_{CH} = 50.7, C≡CH), 65.0 (d, ¹*J*_{CH} = 250.7, C≡CH); 11, 111.5 (s, ReC≡C), 96.7 (d, ²*J*_{CP} = 17.0, ReC≡C), 70.9 (q, ²*J*_{CH} = 11.1, C≡CCH₃), 68.9 (br m, C≡CCH₃); 8, 112.2 (s, ReC≡C), 106.6 (d, ²*J*_{CP} = 15.8, ReC≡C), 93.6 (d, ⁴*J*_{CP} = 2.1, C≡CSi), 79.7 (br s, C≡CSi); HC≡CC≡CSiMe₃, 88.7 (d, ³*J*_{CH} = 6.2, C≡CSi), 83.9 (decel, ³*J*_{CH} = 2.7, C≡CSi), 69.1 (d, ¹*J*_{CH} = 258.8, HC≡C), 68.9 (d, ²*J*_{CH} = 47.9, HC≡C).

(43) (a) Hölzl, F.; Wrackmeyer, B. *J. Organomet. Chem.* 1979, 179, 397. (b) Kamienska-Trela, K. *Org. Magn. Reson.* 1980, 14, 398.

and solvent was removed by oil pump vacuum. The residue was dissolved in a minimum of THF, and hexane (10 mL) was added. Solvent was removed by oil pump vacuum to give **9** as an orange powder (0.0791 g, 0.119 mmol, 84%), mp 84–86 °C dec. Calcd for $C_{32}H_{31}NOPRe$: C, 57.99; H, 4.71. Found: C, 57.86; H, 4.84. IR (CH₂Cl₂/KBr)³⁷ $\nu_{C=C}$ 3305/3287 m, $\nu_{C=C}$ 2115/2113 s, 1975/1975 w, ν_{NO} 1644/1645 vs. MS (EI, 70 eV)³⁸ 663 (9^+ , 100%); no other peaks above 300 of >20%.

NMR (C₆D₆):³⁷ 1H 7.75–7.65 (m, 6H of 3C₆H₅), 7.07–6.94 (m, 9H of 3C₆H₅), 1.95 (d, $J_{HP} = 1.0$, \equiv CH), 1.57 (s, C₅(CH₃)₅), $^{13}C\{^1H\}$ 135.4 (d, $J_{CP} = 51.4$, *i*-PPh), 134.3 (d, $J_{CP} = 10.9$, *o*-PPh), 130.2 (s, *p*-PPh), 128.3 (d, $J_{CP} = 10.0$, *m*-PPh), 110.8 (s, ReC≡C),⁴² 102.1 (d, $J_{CP} = 15.9$, ReC≡C), 100.5 (s, C₅(CH₃)₅), 72.4 (s, C≡CH),⁴² 65.2 (s, C≡CH), 10.0 (s, C₅(CH₃)₅); $^{31}P\{^1H\}$ 20.9 (s).

(η^5 -C₅Me₅)Re(NO)(PPh₃)(C≡CC≡CLi) (**10**). A Schlenk flask was charged with **9** (0.066 g, 0.100 mmol) and THF (5 mL) and cooled to –45 °C. Then *n*-BuLi (2.5 M in hexane; 65 μ L, 0.150 mmol) was added with stirring. After 2 h, the mixture was concentrated to ca. 1 mL by oil pump vacuum at –10 °C. Hexane (10 mL) was added with stirring. The air and water sensitive orange powder was isolated by filtration (–10 °C) and dried by oil pump vacuum (–10 °C) to give **10** (0.047 g, 0.070 mmol, 70%) that was >98% pure by ³¹P NMR and sometimes showed small amounts of **9** by IR. IR (THF)³⁷ $\nu_{C=C}$ 2081 w, ν_{NO} 1642 vs. $^{31}P\{^1H\}$ NMR (THF)³⁷ 20.9 (s).

(η^5 -C₅Me₅)Re(NO)(PPh₃)(C≡CC≡CMe) (**11**). A Schlenk flask was charged with **9** (0.044 g, 0.066 mmol) and THF (5 mL) and cooled to –80 °C. Then *n*-BuLi (2.5 M in hexane; 30 μ L, 0.075 mmol) was added with stirring. After 1.5 h, MeI (25 μ L, 0.40 mmol) was added. After 1.5 h, the cold bath was removed. After 1 h, solvent was removed by oil pump vacuum. The residue was extracted with benzene (2 \times 5 mL). The extract was filtered through a silica gel pad (1 cm), and solvent was removed by oil pump vacuum. The residue was dissolved in a minimum of THF, and hexane (5 mL) was added. Solvent was removed by oil pump vacuum to give **11** as a yellow-orange powder (0.038 g, 0.056 mmol, 85%), mp 61–65 °C dec. Calcd for $C_{33}H_{33}$ -NOPRe: C, 58.56; H, 4.91. Found: C, 58.29; H, 5.09. IR (CH₂Cl₂/KBr)³⁷ $\nu_{C=C}$ 2193/2194 m, 2027/2029 m, ν_{NO} 1644/1644 vs. MS (EI, 70 eV)³⁸ 677 (11^+ , 100%), 614 ((η^5 -C₅Me₅)Re(NO)(PPh₃)⁺, 31%); no other peaks above 225 of >20%.

NMR (C₆D₆):³⁷ 1H NMR 7.80–7.72 (m, 6H of 3C₆H₅), 7.07–6.92 (m, 9H of 3C₆H₅), 1.81 (s, \equiv CCH₃), 1.61 (s, C₅(CH₃)₅), $^{13}C\{^1H\}$ 135.7 (d, $J_{CP} = 50.6$, *i*-PPh), 134.4 (d, $J_{CP} = 10.2$, *o*-PPh), 130.1 (s, *p*-PPh), 128.3 (d, $J_{CP} = 9.8$, *m*-PPh), 111.6 (s, ReC≡C),⁴² 100.3 (s, C₅(CH₃)₅), 96.8 (d, $J_{CP} = 17.3$, ReC≡C), 71.9 (s, C≡CCH₃), 69.1 (d, $J_{CP} = 3.1$, C≡CCH₃),⁴² 10.0 (s, C₅(CH₃)₅), 4.5 (s, \equiv CH₃); $^{31}P\{^1H\}$ 21.0 (s).

trans-(η^5 -C₅Me₅)Re(NO)(PPh₃)(C≡CC≡C)Pd(PEt₃)₂(C≡CC≡C)(Ph₃P)(ON)Re(η^5 -C₅Me₅) (**12**). A Schlenk tube was charged with **9** (0.068 g, 0.10 mmol) and THF (5 mL) and cooled to –80 °C. Then *n*-BuLi (2.4 M in hexane; 55 μ L, 0.13 mmol) was added with stirring. After 1.5 h, a solution of *trans*-Pd(PEt₃)₂(Cl)₂ (0.022 g, 0.053 mmol) in THF (3 mL) was added by cannula. The cold bath was kept at –80 °C for 1 h, and then allowed to slowly warm to room temperature. After 3 h, solvent was removed by oil pump vacuum, and the residue was extracted with ether (2 \times 10 mL). The extract was passed through a medium-frit Kramer filter, concentrated to ca. 3 mL, and kept at –20 °C. After 24 h, the dark red microcrystals were collected by filtration and dried by oil pump vacuum to give **12** (0.062 g, 0.037 mmol, 73%), mp 165–168 °C dec. Calcd for $C_{76}H_{90}N_2O_2P_4$ -PdRe₂: C, 54.78; H, 5.44. Found: C, 54.55; H, 5.29. IR (CH₂Cl₂/KBr)³⁷ $\nu_{C=C}$ 2114/2114 w, 1984/1988 w, ν_{NO} 1632/1634 vs. Raman (CH₂Cl₂) $\nu_{C=C}$ 2111 s, 2090 s. UV-vis (nm (ϵ , M^{−1} cm^{−1}), 7.3 \times 10^{−6} M CH₂Cl₂) 234 (80000), 268 sh (46000), 308 sh (27000), 388 sh (5000). MS (positive FAB, 3-NBA/benzene)³⁸ 1667 (12^+ , 8%), 1040 ($12^+ - (\eta^5$ -C₅Me₅)Re(NO)(PPh₃)(C₅Me₅), 2%), 780 ((η^5 -C₅Me₅)Re(NO)(PPh₃)(C₄PEt₃)⁺, 100%), 614 ((η^5 -C₅Me₅)Re(NO)(PPh₃)⁺, 11%); no other peaks above 200 of >10%.

NMR (C₆D₆):³⁷ 1H 7.83–7.75 (m, 12H of 6C₆H₅), 7.12–6.96 (m, 18H of 6C₆H₅), 1.82 (m, 2P(CH₂CH₃)₃), 1.67 (s, 2C₅(CH₃)₅), 1.12 (m, 2P(CH₂CH₃)₃); $^{13}C\{^1H\}$ 136.3 (d, $J_{CP} = 50.6$, *i*-PPh), 134.7 (d, $J_{CP} = 10.5$, *o*-PPh), 129.8 (s, *p*-PPh), 128.1 (d, $J_{CP} = 9.8$, *m*-PPh), 117.0 (s, ReC≡C),⁴² 100.5 (t, $J_{CP} = 11.1$, C≡CPd), 100.1 (s, C₅(CH₃)₅), 98.2 (d, $J_{CP} = 3.3$, C≡CPd),⁴² 87.4 (d, $J_{CP} = 18.4$, ReC≡C), 17.8 (virtual

t, $J_{CP} = 14.2$, P(CH₂CH₃)₃), 10.1 (s, C₅(CH₃)₅), 9.0 (s, P(CH₂CH₃)₃); $^{31}P\{^1H\}$ 20.8 (s, ReP), 19.5 (s, PdP).

trans-(η^5 -C₅Me₅)Re(NO)(PPh₃)(C≡CC≡C)Pd(PEt₃)₂(Cl) (**13**).

Method A: Complex **9** (0.068 g, 0.10 mmol), THF (5 mL), *n*-BuLi (2.4 M in hexane; 55 μ L, 0.13 mmol), and *trans*-Pd(PEt₃)₂(Cl)₂ (0.043 g, 0.10 mmol) in THF (3 mL) were combined in a procedure analogous to that for **12**. Solvent was removed after the Kramer filtration by oil pump vacuum. The orange-red powder (0.0964 g) was analyzed by ³¹P NMR, which showed a 24:18:58 *trans*-Pd(PEt₃)₂(Cl)₂/**12**/**13** mol ratio (0.0094 g, 0.023 mmol; 0.0286 g, 0.017 mmol; 0.0584 g, 0.056 mmol, 56%). The sample was dissolved in toluene, layered with hexane, and kept at –30 °C. A 9:91 *trans*-Pd(PEt₃)₂(Cl)₂/**13** mixture slowly precipitated. Several repetitions gave **13** as a red powder, mp 145–148 °C dec. Calcd for $C_{44}H_{60}ClNOP_3$ PdRe: C, 54.78; H, 5.44. Found: C, 54.55; H, 5.29. IR (CH₂Cl₂/KBr)³⁷ $\nu_{C=C}$ 1988/1988 w, ν_{NO} 1632/1634 vs. Raman (CH₂Cl₂) $\nu_{C=C}$ 2128 s, 2093 s. MS (positive FAB, 3-NBA/benzene)³⁸ 1039 (**13**⁺, 7%), 780 ((η^5 -C₅Me₅)Re(NO)(PPh₃)⁺, 100%), 614 ((η^5 -C₅Me₅)Re(NO)(PPh₃)⁺, 10%), no other peaks above 225 of >20%. **Method B:** Complex **9** (0.068 g, 0.10 mmol), THF (10 mL), and *n*-BuLi (2.4 M in hexane; 55 μ L, 0.13 mmol) were combined in a procedure analogous to Method A. The solution was slowly added by cannula to a stirred –80 °C solution of *trans*-Pd(PEt₃)₂(Cl)₂ (0.087 g, 0.20 mmol) in THF (10 mL). An identical workup gave an orange-red powder (0.144 g, ca. 95%) that was a 50:50 *trans*-Pd(PEt₃)₂(Cl)₂/**13** mixture. One precipitation as in Method A gave a 4:96 mixture (0.056 g).

NMR (C₆D₆):³⁷ 1H 7.82–7.76 (m, 6H of 3C₆H₅), 7.11–7.02 (m, 9H of 3C₆H₅), 1.80 (m, 2P(CH₂CH₃)₃), 1.65 (s, C₅(CH₃)₅), 1.07 (pseudoquint, $J \approx 8$ Hz, 2P(CH₂CH₃)₃); $^{13}C\{^1H\}$ 136.6 (d, $J_{CP} = 49.9$, *i*-PPh), 135.0 (d, $J_{CP} = 10.8$, *o*-PPh), 130.3 (s, *p*-PPh), 128.6 (d, $J_{CP} = 9.8$, *m*-PPh), 116.1 (s, ReC≡C),⁴² 100.5 (s, C₅(CH₃)₅), 95.0 (d, $J_{CP} = 3.7$, C≡CPd),⁴² 90.8 (d, $J_{CP} = 17.6$, ReC≡C), 83.9 (t, $J_{CP} = 17.3$, C≡CPd), 16.4 (virtual t, $J_{CP} = 14.0$, P(CH₂CH₃)₃), 10.4 (s, C₅(CH₃)₅), 9.0 (s, P(CH₂CH₃)₃); $^{31}P\{^1H\}$ 20.9 (s, ReP), 18.5 (s, PdP).

trans-(η^5 -C₅Me₅)Re(NO)(PPh₃)(C≡CC≡C)Rh(PPh₃)₂(CO) (**14**). Complex **9** (0.068 g, 0.10 mmol), THF (5 mL), *n*-BuLi (2.4 M in hexane; 55 μ L, 0.13 mmol), and *trans*-Rh(PPh₃)₂(CO)(Cl) (0.0760 g, 0.110 mmol) in THF (5 mL) were combined in a procedure analogous to that for **12**. The cold bath was kept at –80 °C for 1 h, and then allowed to slowly warm to room temperature. After 1 day, a ³¹P NMR spectrum showed ca. 50% conversion to **14**. Various workups afforded only crude product. IR (CH₂Cl₂)³⁷ $\nu_{C=C}$ 2110 w, ν_{CO} 1964 s, ν_{NO} 1636 s. MS (positive FAB, 3-NBA/THF)³⁸ 1317 (**14**⁺, 21%), 1027 (**14**⁺ – PPh₃ – CO, 3%), 627 (Rh(PPh₃)₂, 62%), 614 ((η^5 -C₅Me₅)Re(NO)(PPh₃)⁺, 19%); no other peaks above 500 of >20%.

NMR:³⁷ 1H (CD₂Cl₂) 7.77–7.19 (m, 9C₆H₅), 1.53 (s, C₅(CH₃)₅); $^{31}P\{^1H\}$ (THF) 20.1 (s, ReP), 32.3 (d, $J_{PRh} = 129$, RhP).

Me₃SiC≡CC≡CC≡CCSiMe₃.³² A three-necked flask was charged with HC≡CC≡CCSiMe₃ (1.878 g, 15.37 mmol) and acetone (50 mL) and fitted with a gas dispersion tube and a condenser with a cold finger on top. A Schlenk flask was charged with CuCl (0.152 g, 1.54 mmol) and acetone (20 mL), and TMEDA (78 μ L, 0.51 mmol) was added with stirring. After 0.5 h, stirring was halted, and a grayish solid separated from a blue supernatant. The three-necked flask was immersed in a 35 °C bath, and O₂ was bubbled through the solution. After ca. 5 min, the blue supernatant was added in portions. When the blue color persisted, an IR spectrum was recorded (1.5–2 h for this reaction). No HC≡CC≡CCSiMe₃ was detected (2188, 2034; product 2044),³⁷ nor had any condensed on the cold finger (a function of O₂ flow rate). Solvent was removed by rotary evaporation, and the residue extracted with pentane (100 mL). The extract was washed with aqueous HCl (50 mL, 3 M), which was in turn extracted with pentane (3 \times 20 mL). The combined pentane extracts were washed with aqueous NaCl and dried over Na₂SO₄. Solvent was removed by rotary evaporation, and the residue dissolved in hot MeOH (50 mL). Aqueous HCl (3 M) was added until precipitation was complete. The sample was stored at –5 °C. After 12 h, fine yellow needles of Me₃SiC≡CC≡CC≡CCSiMe₃ were collected by filtration, washed with cold MeOH, dried by oil pump vacuum (1.529 g, 6.396 mmol, 82%), and stored in a freezer. The IR and UV-visible spectra matched those previously reported.^{32a} IR (pentane)³⁷ $\nu_{C=C}$ 2181 w, 2048 s.

NMR:³⁷ ¹H (CDCl₃) 0.19 (s, Si(CH₃)₃); ¹³C{¹H} (THF-*d*₈) 88.0, 87.8 (2 s, C≡CSi, tentative), 68.0, 62.1 (2 s, C≡CC≡CSi, tentative), -0.6 (s, Si(CH₃)₃).

[(η^5 -C₅Me₅)Re(NO)(PPh₃)(Me₃SiC≡CC≡CC≡C-C≡CSiMe₃)]⁺BF₄⁻ (**18**⁺BF₄⁻). Complex **5** (0.252 g, 0.400 mmol), C₆H₅Cl (10 mL), HBF₄·OEt₂ (6.6 M in ether; 73 μ L, 0.48 mmol), and Me₃SiC≡CC≡CC≡CC≡CSiMe₃ (0.34 g, 1.4 mmol; in 5 mL of C₆H₅Cl) were combined in a procedure analogous to that for **7**⁺BF₄⁻. The cold bath was allowed to warm to room temperature. The mixture was monitored by IR (product 2177 w, 2147 w, 2122 w, 1710 vs; precursors 2044 s, 1673 s),³⁷ and after 1–2 days was filtered through a Celite pad (2 cm) into rapidly stirred ether (150 mL). The black-brown precipitate was isolated by filtration, dried by oil pump vacuum, and dissolved in CH₂Cl₂ (5 mL). The solution was added dropwise to rapidly stirred hexane (150 mL). The olive powder was collected by filtration and dried by oil pump vacuum to give **18**⁺BF₄⁻ (0.193 g, 0.195 mmol, 48%; 60:40 mixture of Re-(C≡C) rotamers), mp 78 °C. Calcd for C₄₂H₄₈BF₄NOPReSi₂: C, 53.49; H, 5.13. Found: C, 52.37; H, 5.02. IR (CH₂Cl₂)³⁷ ν _{C≡C} 2166 vw, 2122 vw, 2091 vw, ν _{NO} 1717 vs. MS (positive FAB, tetraglyme/benzene)³⁸ 856 (**18**⁺, 33%), 614 ((η^5 -C₅Me₅)Re(NO)(PPh₃)⁺, 100%); no other peaks above 100 of >10%.

NMR (CD₂Cl₂, two Re-(C≡C) rotamers):³⁷ ¹H 7.79–7.50 (m, 6H of 3C₆H₅), 7.48–7.31 (m, 9H of 3C₆H₅), 1.80/1.77 (2 s, C₅(CH₃)₅, 60:40), 0.27/0.21/0.08/−0.31 (4 s, 2Si(CH₃)₃, 30:19:31:21); ¹³C{¹H} NMR (partial)⁴¹ 112.80/112.65 (2 s, C₅(CH₃)₅, 60:40), 9.84/9.68 (2 s, C₅(CH₃)₅, 60:40), −0.53/−0.59/−0.61/−0.68 (4 s, 2Si(CH₃)₃, 20:27:32:21); ³¹P{¹H} 16.0/14.9 (2 s, 40:60).

Cyclic Voltammetry. All voltammograms were recorded in CH₂Cl₂ (freshly distilled from CaH₂ and N₂ purged) that was 7–8 \times 10^{−3} M in substrate and 0.1 M in *n*-Bu₄N⁺BF₄⁻ (crystallized from EtOH/hexane and dried by oil pump vacuum, 75 °C, 24 h). An EG&G Princeton Applied research Model 273 potentiostat (EG&G version 4.0 PARC software) was employed. Cells were fitted with Pt working (1.6 mm diameter) and counter electrodes and an Ag wire pseudoreference electrode. Ferrocene was subsequently added (E° = +0.56 V), and a calibration voltammogram recorded.

ESR. All manipulations were conducted under argon. Schlenk flasks were charged with CH₂Cl₂ (0.5 mL; freshly distilled and

degassed) and **5**, **3**, or **12** (0.11 mmol; 6.9, 11.2, or 18.3 mg). A solution of (η^5 -C₅H₅)₂Fe⁺PF₆⁻ (6.6 mg, 0.20 mmol) in CH₂Cl₂ (1.0 mL) was similarly prepared, and 0.5 mL was added to the solutions of **5**, **3**, or **12** by syringe. After 5–10 s, the mixed samples were transferred by cannula to a 4-mm quartz ESR tube, which was capped with a septum. Spectra were immediately recorded on a Bruker ER 200D-SRC spectrometer in the X-band frequency range (ambient temperature), with a modulation frequency of 100 kHz. The magnetic field was calibrated immediately after each spectrum with diphenylpicrylhydrazide (g 2.0035 \pm 0.0002) external standard, without changing the frequency of the microwave bridge.

A dark red cube was obtained by slowly cooling a hexane solution of **3**. Data were collected as outlined in Table 1. Cell constants were obtained from 25 reflections with 20° < 2θ < 30°. The space group was determined from systematic absences (h0l, h + l = 2n + 1; 0k0, k = 2n + 1) and subsequent least-squares refinement. Lorentz, polarization, and empirical absorption (Ψ scans) corrections were applied. The structure was solved by standard heavy-atom techniques with the SDP/VAX package.⁴⁴ Non-hydrogen atoms were refined with anisotropic thermal parameters. One carbon of a P2 ethyl group showed a slight conformational disorder. Hydrogen atom positions were calculated and added to the structure factor calculations, but were not refined. Scattering factors, and $\Delta f'$ and $\Delta f''$ values, were taken from the literature.⁴⁵ Atomic coordinates and other data can be located in the supporting information.^{10a}

Acknowledgment. We thank the DOE for support of this research, Dr. J. W. Seyler for preliminary electrochemical data, and Dr. W. Cantrell, Jr., for help with the preparation of Me₃SiC≡CC≡CC≡CC≡CSiMe₃.

JA952575F

(44) Frenz, B. A. The Enraf-Nonius CAD 4 SDP—A Real-time System for Concurrent X-ray Data Collection and Crystal Structure Determination. In *Computing and Crystallography*; Schenk, H., Olthof-Hazelkamp, R., van Koningsveld, H., Bassi, G. C., Eds.; Delft University Press: Delft, Holland, 1978; pp 64–71.

(45) Cromer, D. T.; Waber, J. T. In *International Tables for X-ray Crystallography*; Ibers, J. A., Hamilton, W. C., Eds.; Kynoch: Birmingham, England, 1974; Vol. IV, Tables 2.2B and 2.3.1.